Zeitschrift: Schweizerische mineralogische und petrographische Mitteilungen = Bulletin suisse de minéralogie et pétrographie

Band: 71 (1991)

Heft: 3

Artikel: Columbite (Fe,Mn)(Nb,Ta)2O6 in the pegmatites of the calc-alkaline Bergell intrusion (southest Central Alps)

Autor: Wenger, Marc / Armbruster, Thomas

DOI: https://doi.org/10.5169/seals-54370

SCHWEIZ. MINERAL. PETROGR. MITT. 71, 349–369, 1991

Columbite $(Fe,Mn)(Nb,Ta)_2O_6$ in the pegmatites of the calc-alkaline Bergell intrusion (southeast Central Alps)

by *Marc Wenger* and *Thomas Armbruster*[1]

Abstract

X-ray fluorescence analyses of rock samples, microscopy of thin sections and field relations were used to classify the pegmatites in the Bergell Alps. Electron microprobe analyses, X-ray single crystal structure refinements, microhardness and optical reflectance determinations were applied for the investigation of associated columbites. Acid dykes of the Bergell intrusion are only slightly differentiated but can be classified according their degree of alkali fractionation. A rare mineral bearing pegmatite type rich in albite and muscovite is distinguished from a biotite type with less albite. Columbite can be found either in a feldspar-quartz matrix or intergrown with garnet, tourmaline and/or beryl of the first type. All columbites show a similar chemical composition of ferrocolumbite with Mn/Fe ≤ 1 and a high degree of cation ordering (> 85%). Such highly ordered ferrocolumbites from pegmatites have not been reported hitherto. A slow postmagmatic cooling rate and the low Sn content seem to be responsible for the high degree of cation ordering in the columbites of the Bergell pegmatites.

Keywords: Bergell (Bregaglia), pegmatite, geochemistry, columbite, crystal structure, crystal chemistry.

Introduction

Columbite is a common mineral in highly differentiated pegmatites. Minerals of the columbite-tantalite group have the general formula AB_2O_6, where typically A: Fe^{2+}, Mn^{2+}; B: Nb^{5+}, Ta^{5+} and crystallize in the space group Pbcn with $\underline{a}$ = 14.3, $\underline{b}$ = 5.7, $\underline{c}$ = 5.1 Å, Z = 4. The structures of these minerals can be interpreted as ordered superstructures of brookite (TiO_2) with $2(Nb,Ta)^{5+}$ + $1(Fe,Mn)^{2+}$ <–> 3 Ti^{4+}. In contrast, $FeTa_2O_6$ belongs to the tetragonal tapiolite series which is related to the rutile structure. Ixiolite and wodginite (Ferguson et al., 1976) are also related to columbite as they have a corresponding oxygen arrangement with the same occupied octahedral sites, but a different ordering pattern of A and B cations. Ixiolite can be described as a columbite substructure (space group Pbcn, $\underline{a}$ = 4.74, $\underline{b}$ = 5.73, $\underline{c}$ = 5.16 Å, Z = 4) with a random distribution of A and B cations (Nickel et al., 1963). A recent review of oxide minerals of niobium and tantalum is given by Černý and Ercit (1989).

The existence of Nb- and Ta-mineralizations in the pegmatites of the Bergell intrusion was first reported about 20 years ago, when columbite crystals were found in pegmatites in the Val Bondasca area (Maurizio and Lareida, 1975) and in pegmatitic boulders in Val Forno (Maurizio and Schatz, 1973). Since then columbite has been collected at several localities. Especially the dykes in Val Codera and near Tanno (Chiavenna) supplied beautiful crystals (Gramaccioli, 1978), but columbite still remains a very rare mineral.

A first inspection of columbite samples from museums and private collections revealed that several "supposed" columbites are in fact minerals of the epidote group (allanite) or other Nb–Ta bearing phases (e.g. Nb-rutile). Furthermore, no crystal chemical description of the columbites of the Bergell intrusion has been reported. The aim of this study is to present an overview of the crys-

[1] Laboratorium für chemische und mineralogische Kristallographie, Universität Bern, Freiestr. 3, CH-3012 Bern, Switzerland.

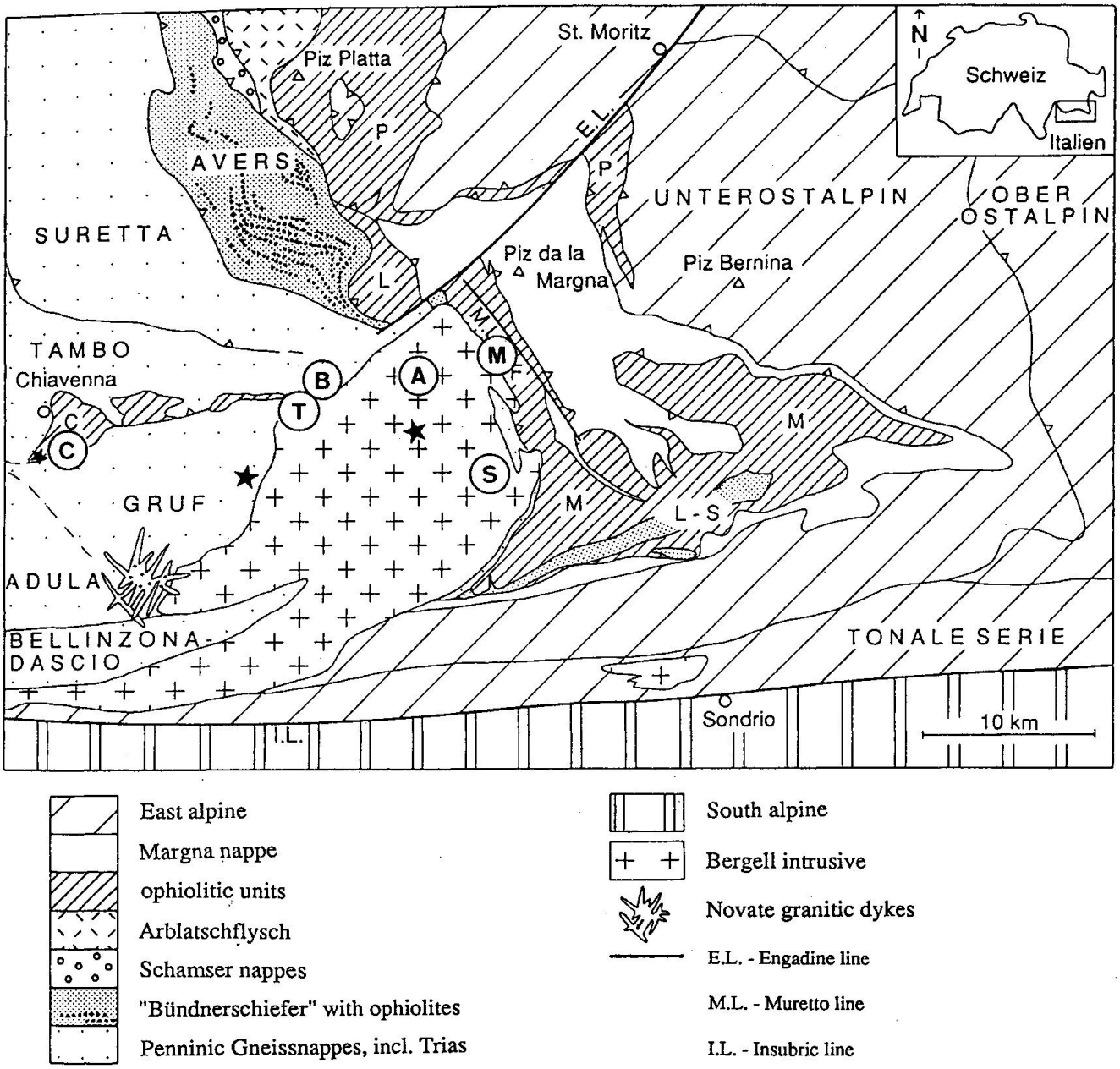

Fig. 1 Tectonic sketch of the Bergell Alps after GUNTLI and LINIGER (1989). Letters surrounded by circles mark the sample locations according table 1. Stars represent further columbite findings (pers. comm. from different collectors and GRAMACCIOLI, 1978).
C = Chiavenna ophiolite; M = Malenco serpentinite; F = Forno unit; P = Platta nappe; L-S = Lanzada-Scermendone zone; L = Lizun.

tal chemistry of the columbite mineralization in these pegmatites and their geochemical environment. Due to a lack of available geochemical data on the columbite bearing pegmatites, an investigation of the dykes was also carried out.

Geologic and petrologic setting

The Bergell intrusion is located at the Swiss-Italian border in the southeast corner of the Central Alpine metamorphic area. It is surrounded by Penninic nappes and in the south by Austroalpine units (Fig. 1). The Bergell batholith is a deep-seated igneous body which intruded in Oligocene times (VON BLANCKENBURG, 1990). The massif consists of zoned structures with granodiorite "ghiandone" at the center surrounded by tonalite "serizzo". The chemical character of the suite is calc-alkaline, including rocks from cumulatic hornblendites and pyroxenites, gabbros, tonalites, granodiorites, aplites and pegmatites (REUSSER, 1987; DIETHELM, 1989). Most of the rocks are deformed and the contacts between granodiorite and tonalite are gradational. A recent geochemi-

Tab. 1 List of rock samples.

Nr.	sample description (locality, altitude a.s.l.)	CH-coordinates
	Val Bondasca	
B-NG1	Gruf-gneiss in contact to pegmatite B-P2 (rock-slide 1972, 1420)	765800/131900
B-P2	Gr-Sch bearing Mu-Fsp-Qz-pegmatite (dito B-NG1)	
	Vallun da la Trubinasca	
T-PNG1-P	Bi- pegmatite in Gruf-migmatite (entrance of canyon, 1400)	764700/131900
T-PNG2-NG	Gruf-migmatite in contact to T-PNG2-P (stream-junction, 1740)	764650/131200
T-PNG2-P	Bi-bearing Mu-Gr-pegmatite in Gruf-migmatite (dito T-PNG2-NG)	
T-PNG4-P	Gr-Sch-Mu-pegmatite in Gruf-migmatite (near T-PNG2-P)	
	Val d'Albigna (Vadrec dal Cantun)	
A-PNG2-P	Coarse-grained Mu-pegmatite in granodiorite (E rock-crest, 2790)	772500/133100
A-PNG3-NG	Fine-grained granodiorite in contact to A-PNG2-P (dito A-PNG2-P)	
A-A1	Bi-bearing aplitic zone in A-PNG2-P (dito A-PNG2-P)	
	Valle Sissone	
S-PNG2-NG	Fine-grained granodiorite (rock-crest E M.Sissone, 2810)	775900/129200
S-PNG2-P	Coarse-grained Bi-pegmatite in S-PNG2-NG (dito S-PNG2-NG)	
	Passo del Muretto (E-Flank Pizzi dei Rossi)	
M-PNG1-NG	Two-mica-gneiss in contact to M-PNG1-P (N firn, 2760)	776300/135200
M-PNG1-P	Gr-Mu-pegmatite in M-PNG1-NG (dito M-PNG1-NG)	
M-PNG2-NG	Amphibolite in contact to M-PNG2-P (rock-crest, 2880)	776000/135000
M-P1	Gr-Mu-aplite to pegmatite in M-PNG2-NG (dito M-PNG2-NG)	
	Chiavenna (Val Schiesone)	
C-P2	Unzoned Bi-bearing Fsp-pegmatite (stream-bed, 520)	751800/129700
C-NG1	Amphibolite in contact to C-P2 (dito C-P2)	
	Chiavenna (Tanno)	
	Profile through wallrock and zoned pegmatite (ravine, 430)	751400/131150
C-NG2-P1	Hanging wall amphibolite	
C-P9-P2	Bi-Mu-Fsp contact zone	
C-P10-P3	Gr-aplitiic zone	
C-P11-P4	Assimiliated amphibolitic scholle	
C-P12-P5	Coarse-grained Gr-Mu-zone	
C-P13-P6	Aplitic contact zone	
C-NG3-P7	Foot wall amphibolite	
	Chiavenna (Prata)	
C-P16	Mu-rosettes zone in pegmatite (rock-crest, 480)	751300/130200
C-P14	Coarse-grained Mu-Gr-core in C-P16 (dito C-P16)	
C-NG4	Ultramafitite in contact to C-P16 (dito C-P16)	

Note: Abbreviations: Gr: garnet; Sch: schorl; Mu: muscovite; Bi: biotite; Fsp: feldspar; Qz: quartz.

cal and geochronological study of these rock types is given by VON BLANCKENBURG (1990). A later undeformed peraluminous intrusion, the Novate leucogranite, crosscuts the Bergell batholith and is, according to trace element variations, not related to the main Bergell body (REUSSER, 1987).

Geological maps used for field investigations were published by STAUB (1921), GYR (1967), SCHMUTZ (1976), WENK and CORNELIUS (1977). Recent geological summaries of the Bergell Alps are given by TROMMSDORFF and NIEVERGELT (1983) and WENK (1986).

Only few data on aplites and pegmatites associated with the Bergell complex are available. GYR (1967) gives a short description of the dykes in the eastern part of the massif, whereas MOTICSKA (1970) inspected the western part. SCHMUTZ (1976) investigated the pegmatites in the mafic-

Tab. 2 Rock chemistry: major- and trace-elements.

Nr.	B-NG1	B-P2	T-PNG1 -P	T-PNG2 -NG	T-PNG2 -P	T-PNG4 -P	A-PNG2 -P	A-PNG3 -NG	A-A1	S-PNG2 -NG	S-PNG2 -P	M-PNG1 -NG	M-PNG1 -P	M-PNG2 -NG
Main elements (wt.%)														
SiO2	71.19	75.93	70.85	65.15	74.21	71.30	72.85	69.32	75.34	72.79	74.59	59.88	75.81	49.43
TiO2	0.28	0.03	0.06	0.61	0.03	0.05	0.04	0.28	0.11	0.18	0.04	0.74	0.06	2.20
Al2O3	14.48	14.52	14.82	17.08	14.84	14.93	13.56	15.22	14.53	14.73	13.84	19.39	14.63	15.75
Fe2O3	2.46	0.80	0.51	4.89	0.70	0.68	0.41	1.89	1.05	1.42	0.37	8.08	0.80	11.60
MnO	0.05	0.07	0.01	0.09	0.04	0.02	0.01	0.04	0.02	0.04	0.01	0.28	0.07	0.33
MgO	0.69	0.10	0.16	1.47	0.14	0.15	0.10	0.62	0.17	0.35	0.10	2.85	0.16	6.16
CaO	1.75	0.63	0.93	3.84	0.48	0.51	0.26	1.92	0.84	1.34	0.28	1.61	0.43	7.36
Na2O	3.34	6.14	4.00	4.26	3.01	3.42	2.39	3.80	3.31	4.29	2.34	2.21	2.47	3.70
K2O	5.04	1.91	5.92	1.66	4.13	6.50	7.35	4.51	5.00	4.57	8.66	3.93	4.33	2.12
P2O5	0.22	0.14	0.08	0.15	0.13	0.11	0.12	0.11	0.06	0.09	0.04	0.10	0.16	0.21
LOI	0.01	0.09	0.02	0.06	0.19	0.08	0.06	0.07	0.08	0.03	0.02	0.22	0.17	0.11
total	99.51	100.36	97.36	99.26	97.90	97.75	97.15	97.78	100.51	99.83	100.29	99.29	99.09	98.97
Trace elements (ppm)														
Ba	<10	411	823	63	391	<10	<10	574	123	216	170	256	<10	19
Rb	236	105	64	381	148	278	352	210	254	312	497	264	391	516
Sr	36	108	325	66	168	43	30	289	92	117	63	95	16	94
Pb	67	9	<5	81	<5	40	40	34	36	45	58	<5	24	<5
Th	68	<5	<5	94	11	19	18	36	21	34	25	37	31	33
U	72	<10	<10	87	<10	23	26	24	20	24	29	30	36	33
Nb	59	<4	<4	96	<4	21	21	20	29	22	28	32	34	21
Y	43	17	15	46	23	20	19	25	28	25	23	40	32	68
Zr	84	20	184	61	72	29	27	175	67	103	33	146	72	200
V	<10	<10	178	<10	74	<10	<10	25	<10	11	<10	162	<10	321
Cr	140	77	83	198	67	101	102	88	136	69	104	228	128	218
Ni	8	<3	<3	15	<3	<3	3	3	4	5	6	101	10	91
Co	<4	<4	25	<4	6	<4	<4	<4	<4	<4	<4	30	<4	39
Cu	<3	<3	8	<3	<3	<3	<3	<3	<3	<3	<3	75	<3	<3
Zn	30	<7	30	30	33	18	8	40	13	27	<7	190	29	189
Ga	34	13	11	47	11	19	19	24	24	22	23	26	27	17
Sc	<2	<2	23	<2	8	3	2	4	3	2	3	20	3	47

Tab. 2 (cont.)

Nr.	M-P1	C-P2	C-NG1	C-NG2 -P1	C-P9 -P2	C-P10 -P3	C-P11 -P4	C-P12 -P5	C-P13 -P6	C-NG3 -P7	C-P16	C-P14	C-NG4
Main-elements (wt.%)													
SiO2	69.96	68.47	49.40	48.47	74.15	73.40	49.01	75.26	75.47	47.91	75.39	86.28	41.47
TiO2	0.07	0.03	1.26	1.51	0.03	0.03	1.52	0.02	0.03	1.47	0.04	0.03	0.09
Al2O3	16.66	19.23	15.75	16.76	14.58	15.00	16.08	14.76	14.86	16.11	14.58	7.42	2.74
Fe2O3	1.21	0.38	9.93	10.30	0.55	0.88	10.49	0.74	0.56	10.16	0.54	1.44	10.48
MnO	0.26	0.02	0.18	0.16	0.01	0.41	0.16	0.23	0.10	0.15	0.01	0.80	0.24
MgO	0.12	0.10	8.49	7.90	0.10	0.10	7.70	0.10	0.11	7.50	0.12	0.15	41.68
CaO	0.33	3.28	11.60	10.55	0.23	0.53	9.78	0.67	0.73	10.19	0.96	0.32	1.06
Na2O	5.03	7.78	2.78	3.33	3.10	4.57	3.10	5.26	4.88	3.27	5.01	2.14	0.08
K2O	3.48	0.51	0.12	0.24	7.24	4.54	0.93	2.58	3.18	0.20	2.81	1.07	0.01
P2O5	0.10	0.21	0.09	0.09	0.06	0.06	0.13	0.06	0.05	0.11	0.05	0.02	0.01
LOI	0.10	0.02	0.08	0.09	0.04	0.03	0.12	0.06	0.05	0.07	0.04	0.02	1.23
total	97.32	100.03	99.68	99.40	100.09	99.55	99.02	99.74	100.02	97.14	99.55	99.69	99.09
Trace-elements (ppm)													
Ba	<10	<10	<10	<10	<10	<10	<10	<10	<10	<10	<10	<10	<10
Rb	930	14	18	28	508	379	135	329	312	18	167	123	15
Sr	<15	181	146	277	<15	<15	244	<15	<15	260	36	<15	<15
Pb	18	<5	<5	<5	25	<5	<5	7	14	<5	18	<5	<5
Th	24	<5	28	30	10	<5	32	<5	9	21	5	<5	26
U	24	<10	28	27	15	<10	35	15	14	24	13	<10	29
Nb	93	<4	17	18	15	10	18	22	20	15	12	21	19
Y	28	37	42	46	15	14	49	19	18	42	20	38	21
Zr	37	199	101	128	20	40	130	42	38	122	49	28	30
V	<10	<10	254	225	<10	<10	237	<10	<10	200	<10	<10	70
Cr	117	41	286	242	103	104	229	137	94	230	126	216	2496
Ni	18	<3	111	87	7	4	70	6	7	74	4	3	1779
Co	<4	<4	36	35	<4	<4	34	<4	<4	32	<4	<4	101
Cu	<3	<3	70	73	<3	<3	92	<3	<3	53	<3	<3	36
Zn	50	<7	63	70	14	13	69	23	17	66	12	8	74
Ga	48	15	12	15	16	15	13	21	19	13	16	11	7
Sc	<2	<2	41	39	<2	<2	42	<2	<2	36	<2	<2	14

Note: Estimated precision for XRF analyses according to Stern (1972). Li, Be and B were not determined which may explain the low total in main elements of some pegmatite analyses. LOI: Loss of ignition. Sample numbers see Table 1

Tab. 3 Columbite: Electron microprobe analyses and formula.

cmpd.	wt.%	range	std-dev	cat.
	B-1			
Nb_2O_5	54.62	37.50-66.4	15.16	1.52
Ta_2O_5	25.89	13.16-44.87	16.75	0.45
TiO_2	0.75	0.63-0.87	0.12	0.04
SnO_2	0.02	0.00-0.04	0.02	0.00
CaO	0	0	0	0
MnO	8.37	7.37-8.98	0.87	0.44
FeO	10.36	9.59-11.39	0.93	0.54
Sb	0	0	0	0
WO_3	0.39	0.00-0.67	0.35	0.01
total	100.40			3.00
	A-1			
Nb_2O_5	37.75	37.53-38.35	0.52	1.16
Ta_2O_5	42.84	41.64-43.86	1.12	0.79
TiO_2	1.28	1.23-1.32	0.05	0.07
SnO_2	0.04	0.00-0.10	0.06	0.00
CaO	0	0	0	0
MnO	9.20	7.96-10.97	1.57	0.53
FeO	8.08	6.58-9.25	1.37	0.46
Sb	0	0	0	0
WO_3	0.28	0.07-0.48	0.20	0.01
total	99.47			3.02
	M-3			
Nb_2O_5	59.97	58.72-61.52	1.42	1.67
Ta_2O_5	13.74	2.60-2.79	0.82	0.23
TiO_2	2.69	2.60-2.79	0.10	0.12
SnO_2	0.22	0.18-0.29	0.06	0.01
CaO	0	0	0	0
MnO	7.96	7.71-8.25	0.27	0.41
FeO	10.46	10.12-10.74	0.31	0.54
Sb	0	0	0	0
WO_3	1.25	0.939-1.57	0.31	0.02
total	96.29			3.00
	C-4			
Nb_2O_5	61.12	60.28-62.11	0.92	1.66
Ta_2O_5	19.14	17.63-20.31	1.37	0.31
TiO_2	0.91	0.79-1.13	0.20	0.04
SnO_2	0.06	0.00-0.087	0.05	0.00
CaO	0.03	0.02-0.04	0.01	0.00
MnO	8.47	7.72-9.07	0.69	0.43
FeO	10.87	10.38-11.29	0.46	0.54
Sb	0	0	0	0
WO_3	0.55	0.48-0.62	0.07	0.01
total	101.15			2.99

cmpd.	wt.%	range	std-dev	cat.
	C-5			
Nb_2O_5	52.76	50.88-55.37	2.34	1.50
Ta_2O_5	28.00	25.93-29.36	1.82	0.48
TiO_2	0.67	0.62-0.74	0.06	0.03
SnO_2	0.07	0.01-0.15	0.07	0.00
CaO	0	0	0	0
MnO	3.94	3.46-4.76	0.71	0.21
FeO	14.56	13.89-14.96	0.58	0.77
Sb	0	0	0	0
WO_3	0.10	0.00-0.16	0.09	0.00
total	100.10			2.99
	C-6			
Nb_2O_5	57.30	56.46-58.76	1.27	1.58
Ta_2O_5	23.45	22.31-24.82	1.27	0.39
TiO_2	0.90	0.87-0.93	0.03	0.04
SnO_2	0.02	0.00-0.05	0.02	0.00
CaO	0	0	0	0
MnO	8.76	8.65-8.84	0.10	0.45
FeO	10.12	9.80-10.32	0.27	0.52
Sb	0	0	0	0
WO_3	0.31	0.21-0.44	0.12	0.01
total	100.86			2.99
	C-8			
Nb_2O_5	56.05	55.42-56.69	0.90	1.56
Ta_2O_5	23.18	22.26-24.10	1.31	0.39
TiO_2	1.10	1.06-1.15	0.06	0.05
SnO_2	0.06	0.02-0.11	0.06	0.00
CaO	0.01	0.011-0.014	0.00	0.00
MnO	8.24	8.00-8.48	0.34	0.43
FeO	10.90	10.86-10.94	0.06	0.56
Sb	0	0	0	0
WO_3	0.62	0.53-0.70	0.12	0.01
total	100.16			3.00

Note: averages based on three analyses. Formula normalized to six oxygen atoms. Sample numbers see Table 8

ultramafic complex between Chiavenna and Val Bondasca. The Val Codera was examined by De Michele and Zezza (1979) and Vogler (1982) proposed a petrogenetic model of the dyke formation in the Pizzo Trubinasca area. A short review of the pegmatites in the Swiss part of the intrusion is given by Lareida (1981).

Analytical methods

X-RAY FLUORESCENCE

Representative rock samples from columbite bearing pegmatites and adjacent wallrocks (Tab. 1 and 2) were prepared by a sequence of crushing,

Tab. 4 Columbite: Cell parameters.

nr.	a [Å]	b [Å]	c [Å]	V [Å³]
	space group Pbcn (nr. 60)			
B-1	14.317(3)	5.740(2)	5.067(1)	416.4(2)
A-1	14.329(2)	5.747(1)	5.074(1)	417.8(1)
M-3	14.292(2)	5.734(1)	5.077(1)	416.0(1)
C-4	14.309(2)	5.745(1)	5.070(1)	416.8(1)
C-5	14.271(9)	5.724(5)	5.052(3)	412.7(5)
C-6	14.316(2)	5.744(2)	5.073(1)	417.1(1)
C-7	14.251(3)	5.737(2)	5.064(1)	413.9(2)
C-8	14.317(2)	5.745(1)	5.074(1)	417.4(1)

Note: sample numbers see Table 8

mixing, and quartering. This procedure reduced the initial amounts of 1 to 30 kg, depending on the grain size of the rock, to ca. 100 g of material. These splits were then powdered in a tungsten carbide vessel. Major elements were determined on fused glass disks, and trace elements on pellets pressed from whole-rock powder. The XRF analyses were performed with an automatic Philips sequential spectrometer (PW 1450) at the Mineralogical Institute of the University of Fribourg.

ELECTRON MICROPROBE ANALYSES

Electron microprobe analyses were carried out on seven columbite samples with a CAMECA SX50 wavelength dispersive (WDS) microprobe, Nb, Ta, Ti, Sn, Ca, Mn, Fe, W and Sb were determined. An accelerating potential of 15 kV, a beam current of 30 nA and a beam size of approximately 1 μm were used. Natural and synthetic oxides as well as pure elements provided reference intensities. A counting time of 30 sec was used for Nb and Ta and 10 sec for the remaining elements. The raw data were corrected on-line for drift, deadtime, background, using PAP correction programs. The analyses and the formula calculated on the basis of six oxygen atoms are given in table 3.

X-RAY DATA COLLECTION AND REFINEMENT OF COLUMBITE STRUCTURE

Eight columbite samples were examined on an ENRAF NONIUS CAD4 single-crystal diffractometer (graphite-monochromatized MoKα X-ray radiation). Cell dimensions (Tab. 4) were refined from 14 automatically centered reflections with $14° < \Theta < 24°$. Two columbite crystal fragments from different locations (B-1 and C-4) were selected to refine their crystal structure and to determine the degree of cation order-disorder. Data collection was performed at room temperature and reflection intensities were measured in the omega scan mode (Θ limit < 30°). A scan width of ca. 2° was used for B-1, whereas ca. 1.5° was sufficient for C-4. Reflections of the type 0kl with $k \neq 2n$, h0l with $l \neq 2n$ and hk0 with $h + k \neq 2n$ were considered as systematically absent and rejected. Psi scans of four strong reflections showed significant intensity variations, thus an empirical absorption correction had to be applied on both samples.

Data reduction, including background, Lorentz-polarisation and absorption corrections, was performed with the SDP program system (Enraf Nonius, 1983). Reflections allowed under space group Pbcn were employed for the refinement using the atomic coordinates of Grice et al. (1976) and the XTAL2.4 program package (Hall and Stewart, 1988). The larger σ, either from averaging or counting statistics, was used as the standard deviation. Structure factors were weighted ($w = 1/\sigma^2$), applying a $6\sigma(F_{obs})$ cutoff (B-1: 430 reflections > $6\sigma(F_{obs})$; C-4: 424, respectively). Neutral atom scattering factors, as well as real and imaginary parts of anomalous dispersion correction were applied. In a first iteration, the A site was assumed to be pure Fe (simulating Fe, Mn and Ti) and the B site pure Nb. To refine the cation distribution, a compositional constraint according the microprobe analyses (Tab. 3) was introduced, while allowing an interchange of (Nb, Ta) and Fe on the A and B sites. Simultaneously, the displacement parameters of the cation positions were refined anisotropically. Ta was assumed to share positions with Nb. The Nb/Ta ratios determined by electron microprobe analy-

Tab. 5 Columbite: final atomic positional parameters, displacement parameters and site occupancies.

atom	x/a	y/b	z/c	Beq	U_{11}	U_{22}	U_{33}	U_{12}	U_{13}	U_{23}
	B-1									
O1	0.0980(3)	0.1014(6)	0.0654(8)	0.37(6) *						
O2	0.4182(3)	0.1171(7)	0.0970(8)	0.50(6) *						
O3	0.7562(3)	0.1252(7)	0.0854(7)	0.35(6) *						
A	0.0	0.3263(2)	0.25	0.86(2)	0.0101(6)	0.0122(6)	0.0106(6)	0.0	0.0000(4)	0.0
B	0.16209(3)	0.17906(7)	0.74418(7)	0.577(9)	0.0071(3)	0.0077(3)	0.0071(2)	-0.0001(2)	-0.0003(2)	-0.0002(2)
	C-4									
O1	0.0970(3)	0.1022(7)	0.0658(9)	0.53(6) *						
O2	0.4184(3)	0.1176(7)	0.0987(9)	0.67(6) *						
O3	0.7558(3)	0.1244(7)	0.0861(8)	0.51(6) *						
A	0.0	0.3275(2)	0.25	0.73(2)	0.0099(7)	0.0100(6)	0.0077(7)	0.0	0.0002(4)	0.0
B	0.16208(3)	0.17869(7)	0.74394(7)	0.34(1)	0.0058(3)	0.0043(2)	0.0029(3)	0.0002(2)	-0.0004(1)	0.0000(2)

site occupancies:

sample	A site	B site
B-1	14.8(5)% Nb+Ta; 85.2(5)% Fe	92.6(3)% Nb+Ta; 7.4(3)% Fe
C-4	9.6(6)% Nb+Ta; 90.4(6)% Fe	95.2(3)% Nb+Ta; 4.8(3)% Fe

Note: * atoms marked by asteriks were refined isotropically.
Displacement parameters are of the form $\exp(-2\pi^2 U_{11}h^2a^{*2}+U_{22}k^2b^{*2}+U_{33}l^2c^{*2}+2U_{12}hka^*b^*+2U_{13}hla^*c^*+2U_{23}klb^*c^*)$. The isotropic displacement factor equivalents (Beq) were calculated according to Hamilton (1959); the standard deviation of Beq was estimated according to Schomaker and Marsh (1983). Sample numbers see Table 8

Tab. 6 Selected interatomic distances (Å) and angles (°).

	B-1	C-4		B-1	C-4
A-O(1) (2x)	2.124(4)	2.112(4)	B-O(1)	1.921(4)	1.929(4)
A-O(2) (2x)	2.138(4)	2.142(4)	B-O(1)	2.062(4)	2.070(4)
A-O(2) (2x)	2.182(4)	2.175(4)	B-O(2)	1.802(4)	1.800(4)
	<2.148>	<2.143>	B-O(3)	1.956(4)	1.955(4)
			B-O(3)	2.063(4)	2.069(4)
O(1)-A-O(1)	105.1(2)	104.6(2)	B-O(3)	2.272(4)	2.271(4)
O(1)-A-O(2) (2x)	95.3(2)	95.6(2)		<2.013>	<2.016>
O(1)-A-O(2) (2x)	95.3(2)	94.8(2)			
O(1)-A-O(2) (2x)	87.4(1)	87.8(2)	O(1)-B-O(1)	88.8(2)	88.5(2)
O(2)-A-O(2) (2x)	83.4(2)	83.6(2)	O(1)-B-O(2)	101.4(2)	100.7(2)
O(2)-A-O(2) (2x)	83.2(2)	83.4(2)	O(1)-B-O(3)	95.1(2)	95.2(2)
O(2)-A-O(2)	80.2(2)	79.9(2)	O(1)-B-O(3)	75.3(2)	75.8(2)
			O(2)-B-O(1)	92.4(2)	92.3(2)
			O(2)-B-O(3	104.4(2)	104.1(2)
			O(2)-B-O(3)	97.1(2)	97.5(2)
			O(3)-B-O(1)	77.3(2)	77.6(2)
			O(3)-B-O(1)	78.2(1)	78.5(2)
			O(3)-B-O(3)	93.0(2)	93.1(2)
			O(3)-B-O(3)	85.4(2)	85.5(2)
			O(3)-B-O(3)	84.3(2)	84.1(2)

Note: sample numbers see Table 7

ses were introduced in the model, leading to an R_w* value of 2.5% for sample B-1 and 2.9% for C-4, respectively. Cell parameters are given in table 4. Table 5 summarizes the final structural parameters. A list of observed and calculated structure factors may be obtained from the authors upon request. Selected interatomic distances and angles are given in table 6.

MICROHARDNESS AND REFLECTANCE

The microhardness (VHN) and the reflectance were measured on the same columbite crystal fragments used for microprobe analyses. Hardness was determined with a Leitz Durimet 2 device using a 981 mN (100 p) load. Results (Tab. 7) are arithmetic mean values of ten measurements. Moh's hardness is calculated from VHN using the correlation equation of HÖLZEL (1989). Reflectance was measured in air (objective 45 : 1; A = 0.85, wavelength 546 nm) and standardized on tungsten carbide (standard WC-011). The limits of five measurements are given in table 7.

Geochemistry of the pegmatites and adjacent wallrocks

FIELD RELATIONS

Late genetic dykes and lenses can be observed all over the intrusion and the neighboring units (see LAREIDA, 1981, his Fig. 2). They show strong variations in general appearance and mineralogy. Microgranitic stocks, several 100 m in size, occur at the NE of the main Bergell body (Monte del Forno). Aplites and pegmatites become the main late genetic formations towards the center of the batholith. Dykes are more frequent in the granodiorite than in the tonalite. The age relation between the different dyke types is not uniform. Pegmatites and aplites crosscut each other without showing distinct generations. The rare quartz-veins are the youngest formation as they crosscut both pegmatites and aplites.

Pegmatites in granodiorites

The dykes intruded into granodiorite (Val d'Albigna, samples A-PNG2-P and A-A1) range

* Note: $R = (\Sigma \| F_{obs} | - | F_{calc} \|) / (\Sigma | F_{obs} |)$; $R_w = \{(\Sigma w(| F_{obs} | - | F_{calc} |)^2) / (\Sigma w | F_{obs} |^2)\}^{\frac{1}{2}}$

Tab. 7 Columbite: sample locations and physical properties.

nr.	locality	assoc. rock	VHN	Moh's hard.	R (%) in air
B-1	Val Bondasca	B-P2	789	6.1	16.6-17-1
A-1	Val d'Albigna	A-PNG2-P	nd	nd	nd
M-3	Passo del Muretto	M-P1	nd	nd	nd
C-4	Chiavenna, Tanno	C-P12-P5	880	6.4	17.2-17.5
C-5	"	"	610	5.6	17.1-17.3
C-6	"	"	816	6.2	16.3-17.0
C-7	"	"	nd	nd	nd
C-8	"	"	756	6.0	16.3-16.9

Note: VHN (microhardness): Leitz Durimet 2, 981 mN (100p). Reflectance: Objective 45:1, wavelength 546 nm. nd: not determined. Rock sample numbers see Table 1

in thickness from several cm up to a few m. The contact to the wallrock is sharp and some of the pegmatites show an internal zoning, characterized by variations in grain size. Common are two zonings: the first type includes aplitic borders and pegmatitic cores, whereas the second type is characterized by an asymmetrical zoned texture. Deformation is present in all dykes, but increases towards the northern contact of the intrusion. Columbite crystals are very rare in this area (sample A-1) and occur only in crystals up to several mm diameter in the coarse-grained parts of the pegmatites.

Pegmatites in Gruf-migmatites

In the Gruf-migmatites (Val Bondasca and Vallun da la Trubinasca, samples B-NG1 and T-PNG1-P) the dykes are of similar thickness and strike E–W, preferred parallel to the local foliation. The contact to the wallrock changes from sharp in the thicker parts to streaked in the thinner parts, where the pegmatites end in schlieren structures. Apophysic off-shooting tongues and assimilation of Gruf-migmatite is common. Very thin garnet strings mark fluidal structures. Zonation is correlated with these flow textures. The dykes are deformed and the coarser pegmatitic zones bear columbites up to 1 cm in diameter.

Pegmatites in the mafic-ultramafic complex

The largest dyke systems can be found in the mafic-ultramafic complexes near Chiavenna and between Passo del Muretto and Val Malenco. As already reported by SCHMUTZ (1976), pegmatites in ultramafitites of the Chiavenna area are different compared to those in amphibolites. Type 1 dykes in ultramafitites form layers up to 25 m thick, without any splitting of secondary dykes, whereas type 2 dykes in amphibolites split up in a large number of smaller branches (SCHMUTZ, 1976, his Fig. 20). In the second type (Chiavenna, Val Schiesone and Tanno, samples C-P2, C-P9-P2 till C-P13-P6) unrotated amphibolite-schollen and fluidal structures are common. Zonation in grain-size and mineralogy is lenticular (Fig. 2), whereas the first type is layered and shows no internal deformation (Chiavenna, Prata, samples C-P14, C-P16). The contact to the wall rock and the amphibolite schollen is in both types very sharp and no reactions can be observed. The most beautiful and largest columbite crystals (up to several cm in diameter) have been found in these dykes (esp. in Chiavenna, Tanno), again in the coarse-grained zones. The dykes in the Muretto-amphibolites (samples M-PNG1, M-P1) are of the same appearance (Fig. 3). They are slightly smaller and show local miarolithic cores. Fluidal structures are well developed (Fig. 4).

The strike direction of the investigated dykes is dependent on the local structures and the rheology of the adjacent rocks. Brittle wallrocks (ultramafites near Chiavenna) lead to thick layers, whereas ductile rocks (amphibolites near Chiavenna, Gruf migmatites in Val Bondasca and Vallun da la Trubinasca) split up the pegmatites in secondary dykes and stocks. The internal deformation increases from the center to the border of the intrusion. Therefore, the plasticity of the wallrock and the local stress during intrusion must be responsible for the appearance of the dykes. With exception of the Gruf-migmatites, the contact to the wallrock is very sharp and no reaction zone is visible. Aplitic zones are more frequent in thinner dykes than in thicker ones. Nevertheless, coarse-grained parts of the pegmatites are also common in contact to the wallrock (Fig. 2). Asymmetrically zoned textures, lense shaped and layered zonations as well as the fluidal structures

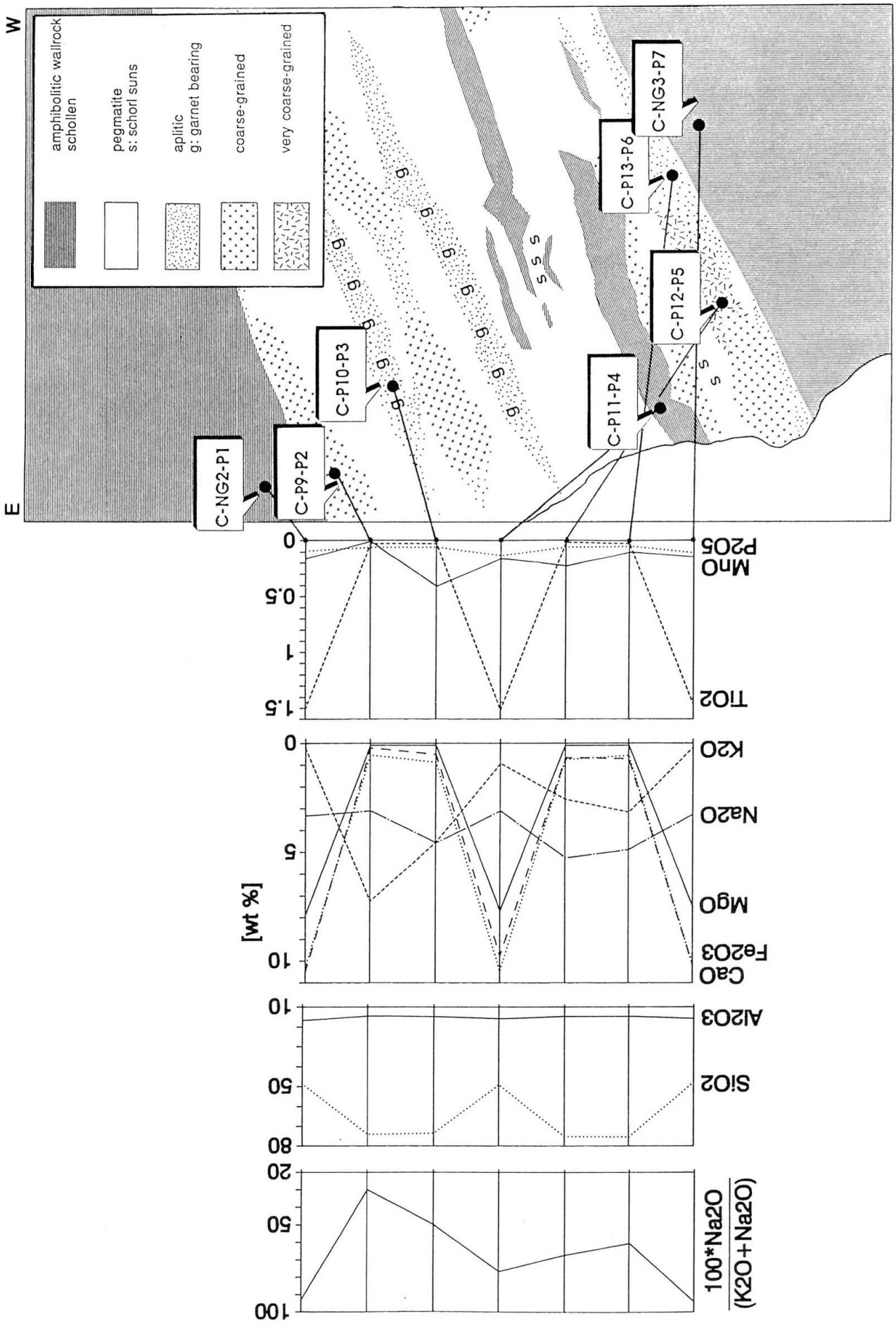

Fig. 2 Mineralogical and geochemical profile (XRF data from table 2) of a pegmatitic dyke near Tanno (Chiavenna, CH-coordinates 751 400 / 131 150).

Fig. 3 Pegmatitic dyke in amphibolite. Dyke thickness is ca 1 m. E-flank Pizzi dei Rossi. Sample locality M-P1 and M-PNG2-NG.

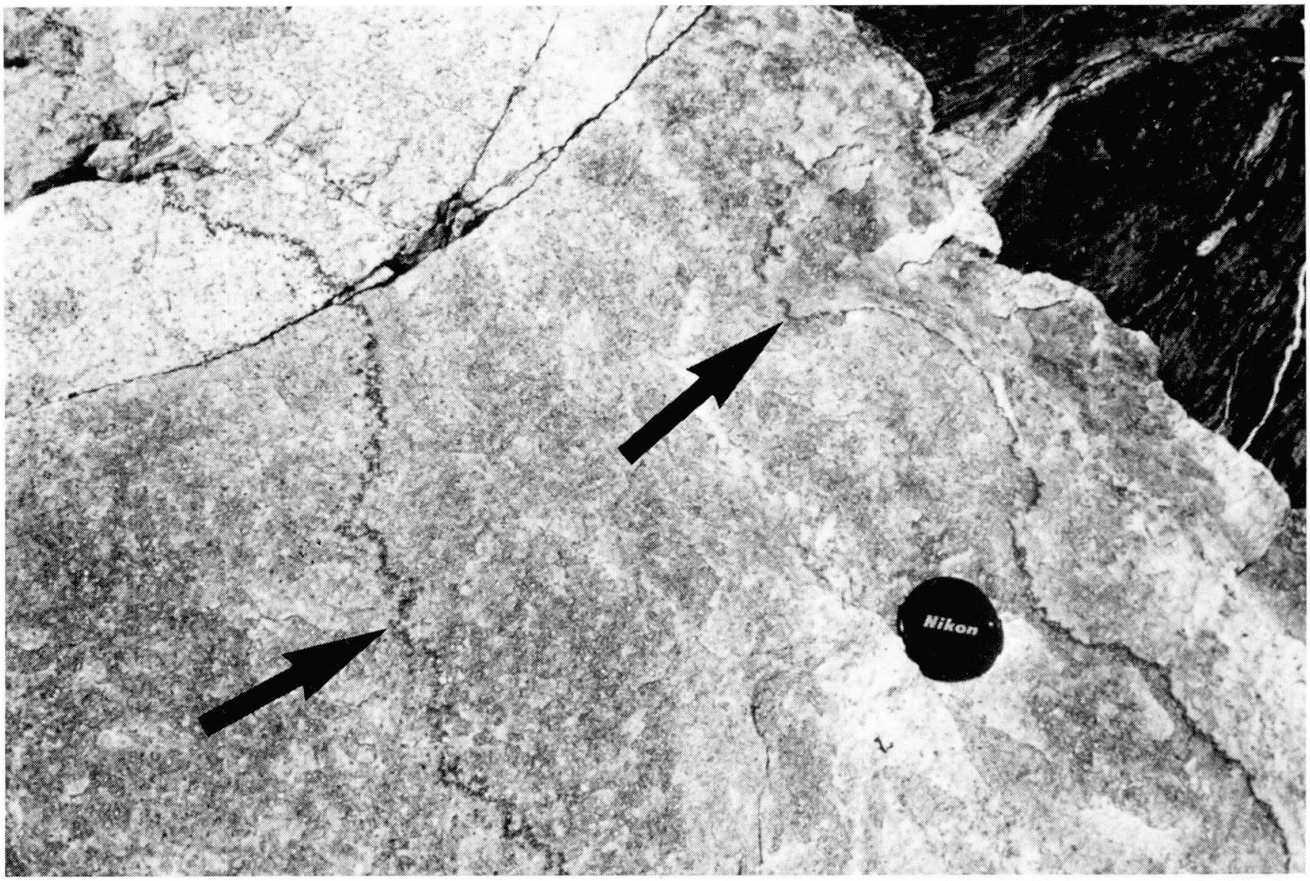

Fig. 4 Detail of figure 3 showing the sharp contact to the amphibolitic wallrock and the fluidal structures inside the dyke, marked by thin strings of garnet (arrows).

suggest that the internal zonation of the dykes is a result of multiple injection and a slow cooling rate. Large temperature differences between dyke and wallrock (VOGLER, 1982) could not be confirmed.

MINERALOGY AND CLASSIFICATION

The main components of the late genetic formations are similar throughout the Bergell complex. In contrast to the main granite body, microgranites (Monte del Forno) bear microcline as the dominant alkali feldspar. Zoned plagioclase (An 10–30) and undulatory quartz are further main components. Biotite and muscovite are both present, in general muscovite is the main mica. Aplitic leucogranitic dykes and stocks are distinguished from the microgranites by their finer grainsize and excess muscovite. For detailed description the reader is referred to WENK (1986), DE MICHELE and ZEZZA (1979), WENK et al. (1977), SCHMUTZ (1976) and GYR (1967).

Several attempts have been made to classify the pegmatites according to their mineralogy. GYR (1967) denied the possibility of distinguishing different pegmatite types in the eastern part of the intrusion. LAREIDA (1981) recognized simple granitic pegmatites in contrast to hybrid pegmatites. Simple granitic pegmatites are differentiation products of the main granitic intrusion, whereas the mineralogy of the hybrids is influenced by assimilation of aluminium-rich wallrocks. These pegmatites bear alumosilicates and cordierites. VOGLER (1982) described zoned and unzoned pegmatites in the Pizzo Trubinasca area. With regard to rare mineral formation, the following classification is introduced (Fig. 5):

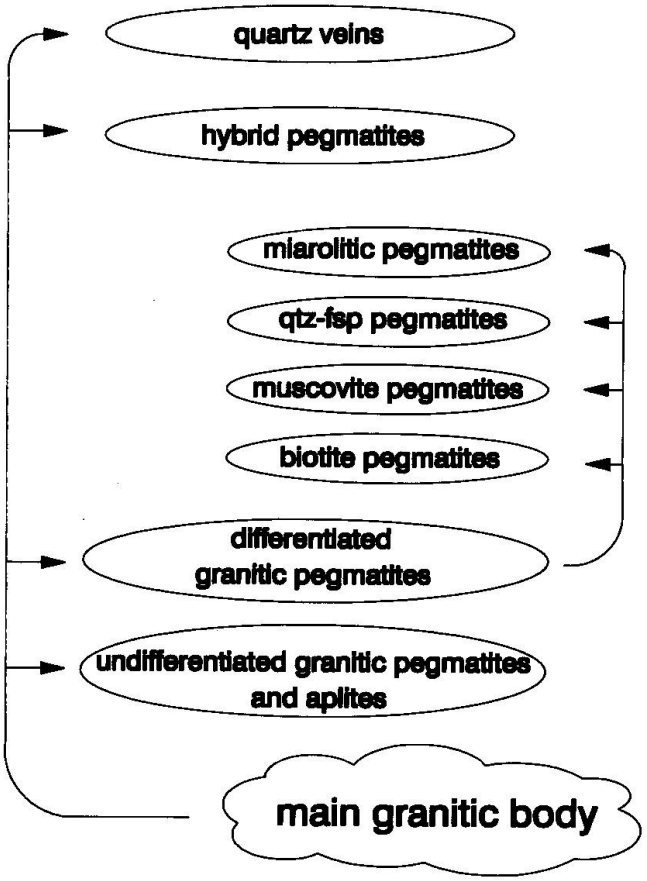

Fig. 5 Classification of the acid dykes of the Bergell intrusion according to their degree of differentiation. See text for explanation.

1. Undifferentiated granitic pegmatites and aplites

This type is very common in the central granitic body and comprises microgranitic and fine-grained leucogranitic dykes. They are of small thickness and differ from the main granite only by an excess of light mica. No columbite has been reported so far.

2. Differentiated granitic pegmatites

This group comprises the rare mineral bearing dykes. According to the trend of increasing differentiation, several subgroups are recognized. The differentiation can occur either laterally, where dykes change their composition as a function of distance from the magma source (Val Bondasca), or as an internal layering due to a slow cooling rate (Chiavenna, Fig. 2). These zonations are often strongly disturbed by effects of multiple injection or late hydrothermal alteration (Pizzi dei Rossi, Figs 3, 4).

2A. Biotite pegmatites – These represent the first stage of differentiation in the sequence. The mineralogy is monotone with plagioclase ≥ alkalifeldspar > quartz > biotite. They are coarse-grained with characteristic biotite flakes up to several cm in diameter disseminated in the feldspar-quartz matrix. The green-brown biotite is locally altered to chlorite and shows a preferred orientation perpendicular to the wallrock contact. Accessories are muscovite, garnet and tourmaline (samples T-PNG1-P, S-PNG2-P, C-P2). Rare minerals are not present.

2B. Muscovite pegmatites – The final volatile enrichment is observed in the muscovite rich pegmatites. The composition is plagioclase > quartz > alkalifeldspar > muscovite. The main

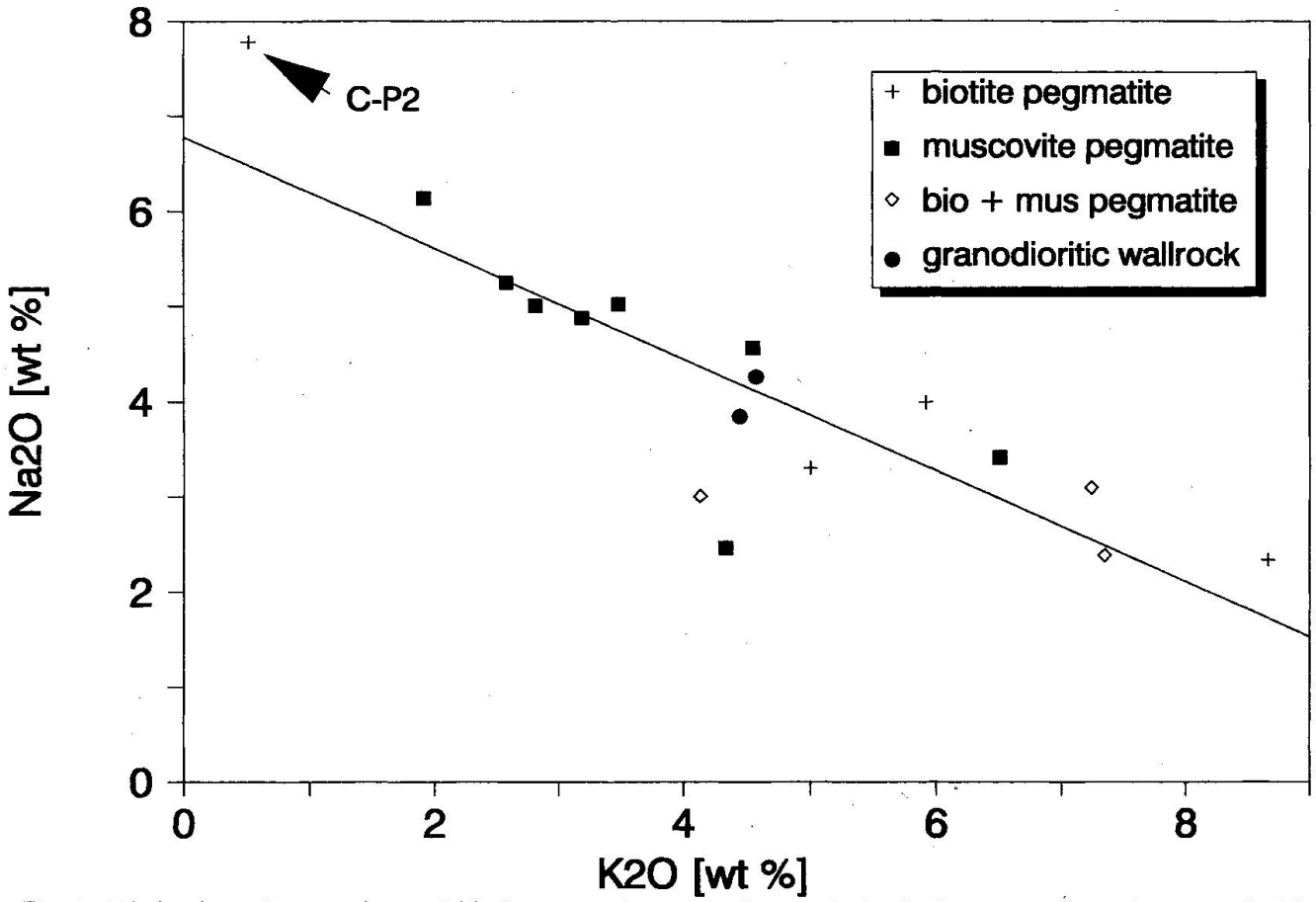

Fig. 6 Distinction of muscovite- and biotite pegmatites according to their alkali content. Note the granodioritic samples (solid circles) which plot between the two pegmatite groups.

component, plagioclase (An 10–30) shows polysynthetic twinning (albite type). Microcline (Ab < 15) is the main alkalifeldspar with coarse perthitic exsolution. Muscovite is light green and disseminated in the feldspar matrix or forms the famous rosettes (Chiavenna, Prata, sample C-P16). Some parts of the dykes are formed by more than 50% of such muscovite aggregates. Important accessory constituents are garnet and tourmaline. The red-brown garnets are idiomorphic and up to 2 cm in diameter, and belong to the spessartine-almandine series with a low pyrope component (VOGLER, 1982). Intergrowths of muscovite and garnet are frequent. Strings of garnet mark the fluidal structures and borders of zones formed by multiple injection. Tourmaline is black and belongs to the schorl-dravite series. Beautiful tourmaline suns are common as well as intergrowths with garnet. In the fine-grained aplitic domains small garnets up to 1 mm in diameter are disseminated in a matrix of feldspar, quartz and muscovite. Most findings of rare minerals are reported from this pegmatite type (samples B-P2, T-PNG4-P, A-PNG2-P and others). Detailed descriptions are reported for beryl (STAUB, 1924; VOGLER, 1982), triplite, zirkon, orthite, dumortierite, cosalite, scheelite, jamesonite, bismuthinite, apatite, molybdenite, ferrimolybdite, monazite, xenotime, magnetite, hematite and columbite (MAURIZIO and LAREIDA, 1975; GRAMACCIOLI, 1978; MAURIZIO and WEIBEL, 1982; VOGLER, 1982).

2C. Quartz-feldspar pegmatites – Graphic textures of quartz and feldspar are frequent at the contact to the wallrock or form the transition from the muscovite zone to a quartz-feldspar core. Columbite (sample C-5) and beryl can be found in these zones, especially at the contact to muscovite and albite enriched domains.

2D. Miarolitic pegmatites – Late hydrothermal alteration can form miarolitic dykes (Pizzi dei Rossi, sample M-P1) with central epidote-chlorite-quartz cores, zeolite mineralization in cavities and local bertrandite formation at the expense of beryl. Columbite seems not to be involved during these alteration processes (sample M-3). The presence of uranium anomalies (e.g. eastern part of Val Bondasca) with the presence of uranium minerals as uraninite or uranyle-hydroxides (becquelerite) in the dykes leads to radiation damage

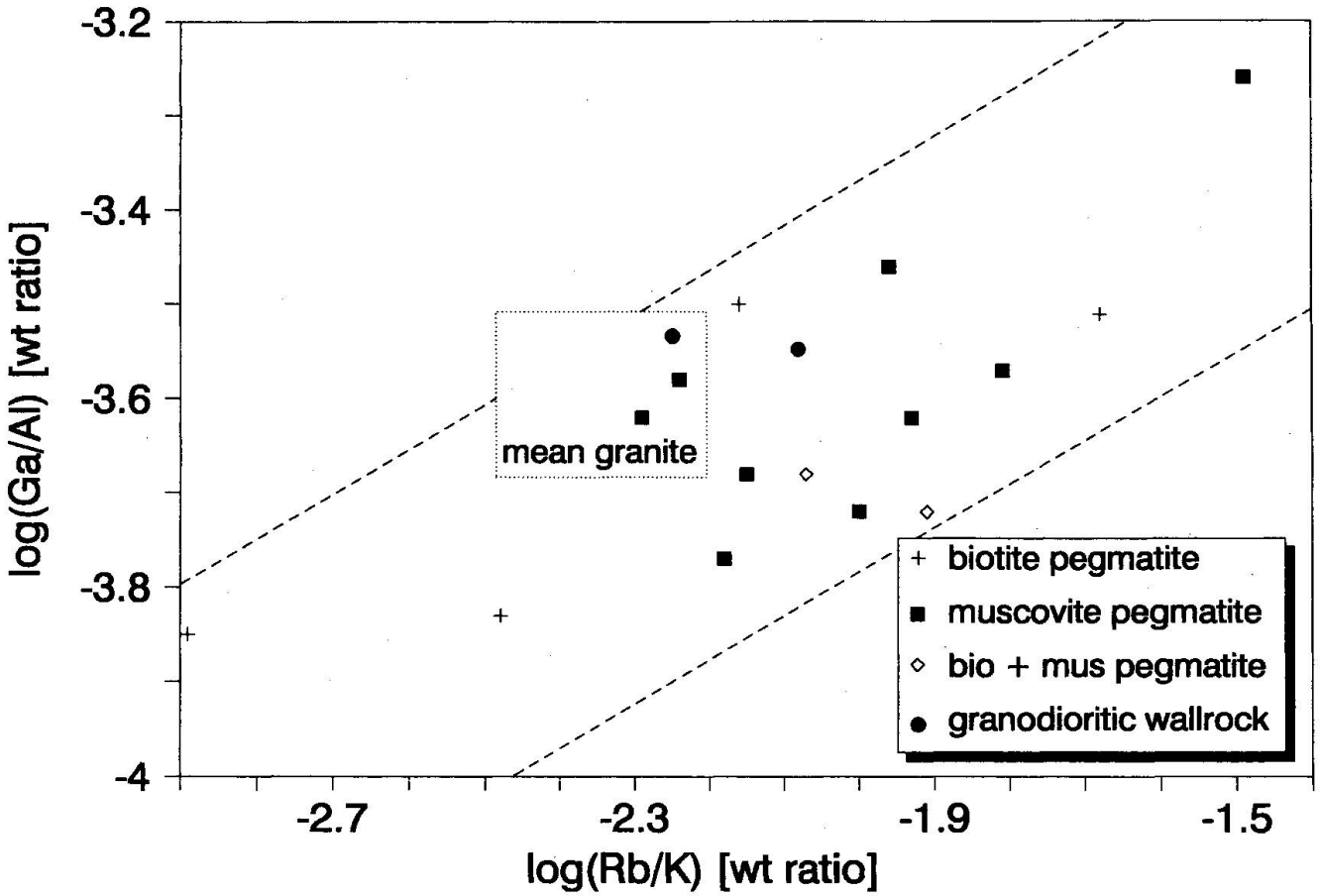

Fig. 7 Ga/Al weight ratio vs Rb/K weight ratio in the pegmatites of the Bergell intrusion. The rectangle marks a mean of granites (MÖLLER, 1989).

in neighboring phases (MAURIZIO and WEIBEL, 1982). Beryl changes its color from light blue to greenish, quartz is dark grey and feldspars become light reddish.

3. Hybrid pegmatites

In this group (LAREIDA, 1981) only dykes with mineralisations clearly induced by assimilation (e.g. andalusite formation in pegmatites in the Fedoz series) should be considered because all dykes show variations in their mineralogy dependent on wallrock chemistry. This can be seen in the pegmatites near Chiavenna, where samples inside ultramafitite bear muscovite and biotite, whereas in the mafitites biotite bearing dykes dominate (SCHMUTZ, 1976). Hybrid pegmatites do not show any important Nb–Ta mineralizations.

4. Quartz veins

They are very rare, they crosscut all above mentioned dyke types and often emanate from the highly differentiated parts of the pegmatites.

Columbite crystals are mainly found in the coarse-grained parts of the muscovite pegmatites, as mentioned above. The largest and best developed crystals are reported from the thickest dykes near Chiavenna (samples C-4 to C-8). Columbite is either paragenetic with plagioclase, microcline, bluish-grey quartz and rarely light mica or it is intensively intergrown with garnet, tourmaline and/or beryl.

GEOCHEMISTRY

The major element composition of pegmatites and adjacent wallrocks is given in table 2. The dykes are distinguished according to their mineralogy, as discussed in the section on field relations (Fig. 5). None of the oxides except of Al_2O_3, Na_2O and P_2O_5, show any differentiation with respect to SiO_2. Only Al_2O_3 tends to decrease with increasing SiO_2. In highly differentiated rocks such as the Bergell pegmatites, fractionation is not reflected in simple relations as e.g. in Harker diagrams. Nevertheless, major element distributions and the chemical profile of the Tanno pegmatite (Fig. 2) show:

a) CaO, Fe_2O_3 and MgO distribution patterns in the amphibolitic wallrock and assimilated schollen inside the pegmatites (C-P11-P4) were not influenced by the intrusion of the dykes;

b) assimilated amphibolitic schollen show variations in the alkali content, compared to the unaltered wallrock;

c) garnet rich parts of the pegmatites are enriched in Mn (sample C-P10-P3);

d) $K_2O > Na_2O$ in biotite pegmatites or biotite zones (C-P9-P2), whereas $Na_2O > K_2O$ in muscovite pegmatites (C-P12-P5).

A significant evolution trend of the pegmatites is reflected in their alkali content. The distinction of muscovite- and biotite-pegmatites according to their field appearance is seen in the Na_2O/K_2O ratio (Fig. 6). A linear correlation (correlation coefficient r = –0.9) exists between the more highly differentiated muscovite pegmatites, rich in Na_2O, and the K_2O rich biotite pegmatites. The granodioritic samples plot between the two pegmatite groups. Outlier C-P2 shows strong alteration, resulting in a high Al_2O_3 content. Aluminum is the only element which decreases significantly with increasing SiO_2. The SiO_2/Al_2O_3 ratio reflects the modal amount of quartz and feldspar. Samples rich in feldspar yield a low SiO_2/Al_2O_3 ratio and vice-versa (see also WENK et al. (1977), their table 2). A comparison of the alkali ratio with the Al_2O_3 content does not disclose any change in the differentiation trend which might be induced by decreasing Al_2O_3. Feldspars are the main alkali bearing phases in the various pegmatite types. Thus, the differentiation trend is manifested in the variation of the albite/microcline ratio. This is in good agreement with thin section observations which show that albite rich plagioclase is the main compound in the muscovite pegmatites, whereas microcline is of minor importance or even missing. In contrast, biotite pegmatites contain as much microcline as plagioclase.

To estimate the degree of differentiation of the pegmatites relative to the main granitic body, fractionation of chemically coherent elements such as Ga/Al, Hf/Zr, Ta/Nb or HREE/LREE must be considered. Extreme differentiation of melts is required to achieve changes of these ratios because of their nearly identical chemical behavior. The Ga/Al ratio is nearly invariable in common magmatic rocks. In highly specialized granites and pegmatites this ratio increases with increasing Rb/K ratio (MÖLLER, 1989). The pegmatites and the granodioritic samples of the Bergell intrusion show a slightly increased Ga/Al ratio of $2.9 \cdot 10^{-4}$ in comparison with "regular" granites with a ratio of $2 \cdot 10^{-4}$ (Fig. 7). All dykes and the granodioritic samples cluster around the regular granite field. Both granodiorite and pegmatites are slightly differentiated with respect to Ga/Al, without any significant difference between the granodiorite and the dykes.

Chondrite-normalized REE patterns of a granodiorite sample from Val Bona and of a pegmatite from Valle Sissone (VON BLANCKENBURG, 1990; his Fig. 1.1.6) reveal a strong depletion of the pegmatites in REE with very large Eu anomalies. The granodiorite shows a similar spectrum with high LREE/HREE enrichment as in the pegmatites, but not such a strong depletion. This confirms the slightly higher differentiation of the pegmatites which are in general lower in REE contents than the related granites with a similar Eu anomaly (SIMMONS et al., 1987). A detailed study of REE distribution in columbite, pegmatites and adjacent wallrocks is under investigation.

Columbite

PHYSICAL PROPERTIES

Columbite crystals (space group Pbcn with $\underline{a}$ = 14.3, $\underline{b}$ = 5.7, $\underline{c}$ = 5.1 Å, Z = 4) can be found in pegmatites all over the Bergell intrusion (Fig. 1 and Tab. 3) as described above. They appear as black, flattened and hypidiomorpic orthorhombic crystals with a typical submetallic luster and a visible cleavage parallel to {100}. Size and habit vary widely, but two main types are observed (Fig. 8). Habit one is very tabular and elongated parallel to the $\underline{c}$-axis. Prismatic and pinacoid faces are dominant, whereas rhombic bipyramids are not developed. The second type is massive and shows more faces than type one. Rhombic bipyramids are in general present.

Type one is the dominant habit of columbite paragenetic with feldspar (mainly albite rich plagioclase) and quartz. The crystals appear either as small splinters of a few mm in diameter finely disseminated in the quartz-feldspar matrix (samples A-1, M-3, C-7, Fig. 9), or as {021} and {023} twins which build aggregates up to several cm in size (samples C-4, C-6 and C-8). A very special habit is displayed by sample C-5. It is extremely elongated parallel to the $\underline{c}$-axis with a {110}/{011} ratio of 40. Type two is common when columbite is intergrown with garnet (sample B-1), tourmaline or beryl, forming clusters up to several cm in diameter.

Microhardness and reflectance (Tab. 7) are in the same order of magnitude for all measured samples. The determined VHN values are at the

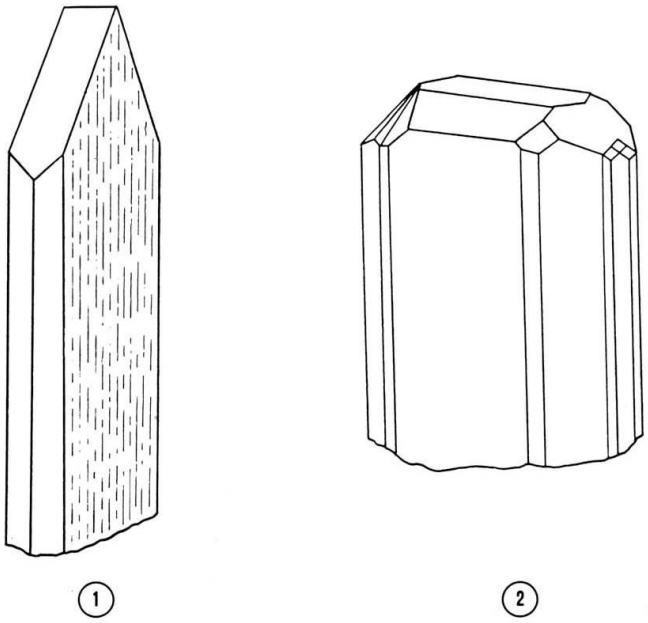

Fig. 8 Sketches of the two main habit types of columbite found in the Bergell pegmatites.
1: Habit one is very tabular and elongated parallel to the c-axis. Prismatic and pinacoid faces are dominant, whereas rhombic bipyramids are not developed.
2: Habit two is massive and shows more faces than type one. Rhombic bipyramids are present in general.
Sketches after GRAMACCIOLI (1978) and TRÖGER (1982).

upper border of the values known for columbites (240–1021), and the reflectance measurements revealed common values (UYTENBOGAARDT and BURKE, 1971). No relationship between chemical composition, reflectance and hardness can be observed. Due to the small grain size of the investigated crystals, the density has not been determined.

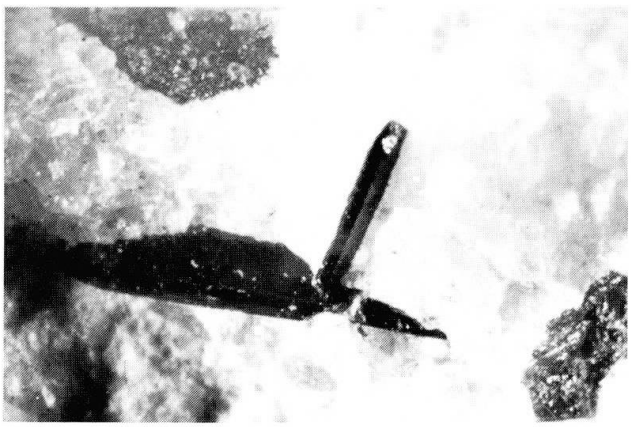

Fig. 9 Columbite crystal of type 1 in feldspar-quartz matrix. Sample M-3 of Passo del Muretto. Length of the crystal at the center is 1.5 mm.

CHEMICAL COMPOSITION

Electron microprobe analyses (Tab. 3) revealed similar chemical compositions for columbites of the Bergell intrusion. In the columbite quadrilateral (Fig. 10) the samples plot in a composition of ferrocolumbite with a high manganese component. Only sample A-1 from Val d'Albigna has Mn > Fe. Therefore A-1 belongs to the group of manganocolumbites. The purest ferrocolumbite end-member is sample C-5 from Chiavenna. This must be considered as a local variation in the chemical composition because the other samples from Chiavenna form a cluster in the columbite quadrilateral. The Bergell columbites show a constant Fe/Mn ratio whereas the Nb and Ta content is variable inside the columbite field. Back-scattered electron images did not reveal significant zoning of the crystals as e.g. observed in columbites from Finland (LAHTI, 1987). Nevertheless, sample B-1 from Val Bondasca shows larger variations in the Nb/Ta ratio, which can be seen in the high standard deviation of the averaged Nb_2O_5 and Ta_2O_5 concentrations in table 3. When columbite is intergrown with garnet (sample B-1) the Mn/Fe ratio in the Nb–Ta phase is close to one (0.8 for B-1), whereas in the garnet of this paragenesis a ratio of 1.4 is observed. Because all columbites show a Mn/Fe ratio close to one, the

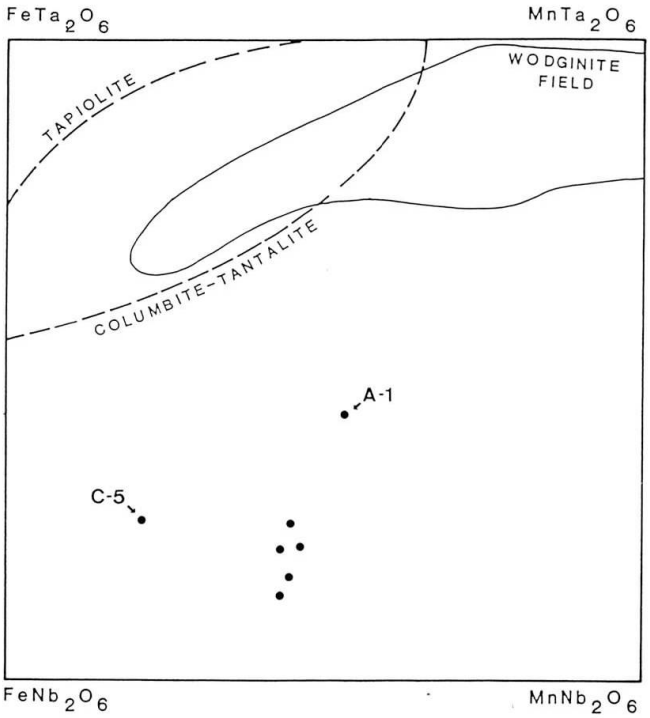

Fig. 10 Compositional range of columbite from pegmatites of the Bergell intrusion (Tab. 4) in the columbite quadrilateral (atomic proportions). Mineral fields and compositional gap separating columbite-tantalite from tapiolite after ČERNÝ and ERCIT (1989).

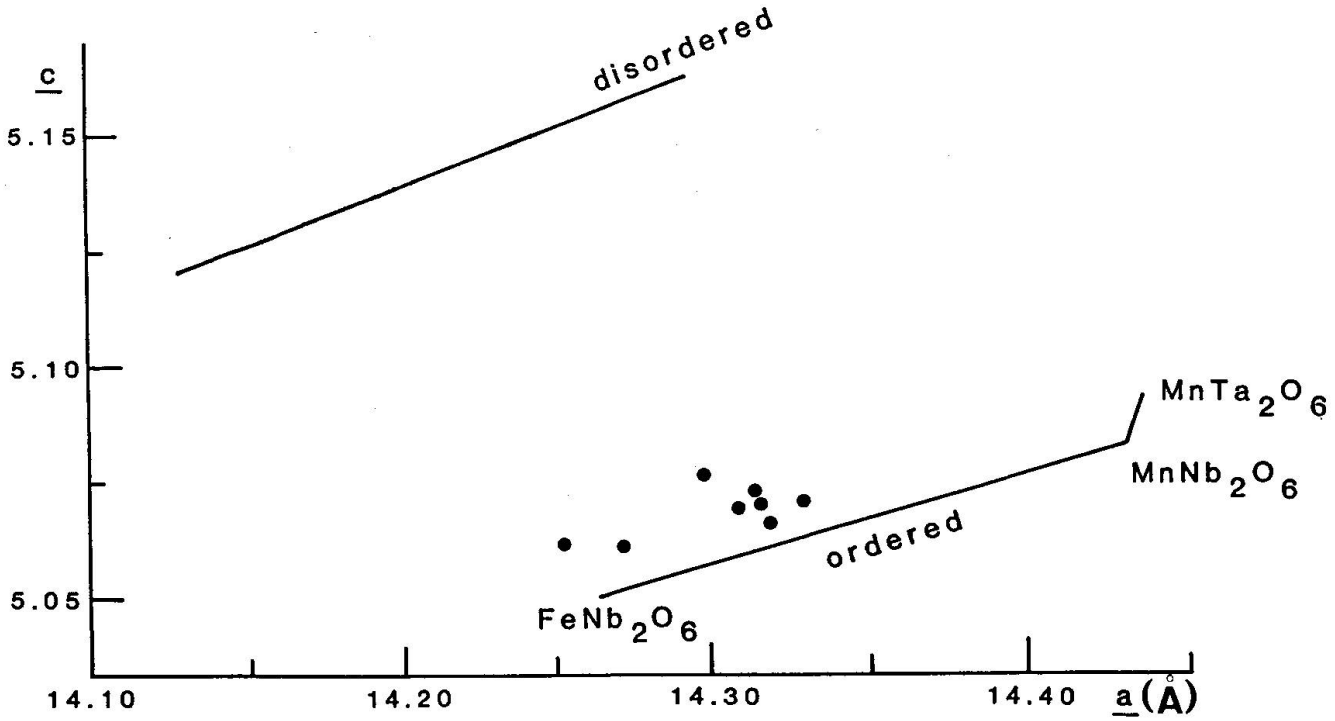

Fig. 11 a-c diagram of columbite from Bergell columbites (Tab. 5) showing the high degree of cation ordering. Ordered-disordered lines after ČERNÝ and ERCIT (1989).

presence of garnet in the paragenesis does not influence the chemical variation in the light transition metals (Mn, Fe) of the Nb–Ta phase. Very minor substitutions by titanium and tungsten are common. Sample M-3 from Passo del Muretto contains significant amounts of both elements, reflected in a lower degree of cation ordering (Fig. 11). The low Sn content in all samples is important, as it may influence the high degree of cation ordering in columbites. PEREGO (1979) reports tantalite from Val Massino and LAREIDA (1981) reports manganotantalite from the Albigna area. However, no analyses of these chemically different specimens have been published.

CRYSTAL STRUCTURE

The small chemical variation of the columbites is also reflected in the corresponding cell parameters (Tab. 4). The high degree of cation ordering in all samples is striking, as represented in the a-c diagram (Fig. 11) adopted from ČERNÝ and ERCIT (1989). A high degree of cation ordering in the columbite structure means a nearly perfect ABBABB stacking of the octahedral layers along the a-axis. In pegmatites, disordered columbites are more common than ordered ones, and minerals of intermediate degree predominate. ČERNÝ and ERCIT (1989) report that, with exception of manganotantalite, highly ordered natural phases in pegmatites are virtually non-existent. Thus, the highly cation ordered ferrocolumbites of the Bergell intrusion seem to be a very rare exception.

Single crystal structure refinement of the two samples B-1 from Val Bondasca and C-4 from Chiavenna, respectively, lead to similar positional parameters (Tab. 5). Site occupancy refinements confirm the high degree of cation ordering. The A site is dominated by the light transition elements (modeled by Fe) (90% in C-4) whereas the B site is favored by Nb + Ta (95% in C-4), leading to 86% ordering for C-4 and 78% for B-1, respectively. The reliability of the site occupancies, refined with the above model, is within 5% (WENGER et al., 1991).

Cation-oxygen distances in the A and B octahedron agree for both samples within 2 σ (Tab. 6). To compare the observed <A–O> and <B–O> distances with those in ordered synthetic columbite with corresponding chemistry, bond lengths from $FeNb_2O_6$, $MnNb_2O_6$, and $MnTa_2O_6$ end members (WEITZEL, 1976, his Tab. 5) were used. Linear interpolation predicts <A–O> distances of <2.144> Å for B-1 and <2.143> Å for C-4, respectively and <B–O> distances: <2.015> Å for B-1 and <2.017> Å for C-4. The predicted distances are in perfect agreement with the observed ones. Columbite with similar chemical composition but low degree of cation ordering can be found in the Kings Mountain pegmatite N.C., U.S.A. <A–O>

distances in this low ordered phase (31% ordering) are significantly shorter (<2.084> Å), whereas <B–O> distances are longer (<2.037> Å) (WENGER et al., 1991, their Tab. 5). Therefore (A,B) cation disorder is also reflected in the mean A–O and B–O distances, confirming the high degree of cation ordering for columbites of the Bergell intrusion.

Discussion

The pegmatites of the Bergell intrusion do not show high differentiation from the main granitic body, whether with respect to main elements, or to the fractionation of chemically coherent elements. However, considering rare element bearing minerals, certain degrees of fractionation and differentiation can be observed. Although the general degree of differentiation is low, enrichment of volatiles and concomitant fractionation of the alkalies leads to the formation of different pegmatite types (Fig. 5). The observed differentiation comprises a discontinuous series with fractionation from biotite to muscovite, together with a continuous increase in the sodium content of plagioclase. During this fractionation the system becomes more and more enriched in quartz at the expense of feldspar, leading to a decrease in Al_2O_3. Thus a less fractionated pegmatite type with microcline > albite and biotite can be distinguished from the higher developed albite-muscovite type. The formation of these groups is not only a function of magmatic differentiation but it is also related to interactions of the pegmatite forming fluid with the wallrock. Metasomatic processes can influence the chemistry, especially the alkali content, of the adjacent wallrock and the pegmatite composition (see the section on mineralogy and classification).

To enable the crystallization of rare element bearing minerals, these incompatible elements must become highly enriched. During this fractionation the partition coefficients are not constant, due to the change in volatile content of the melt and to the amount of complexing agents. These processes are very complex when associated with possible multiple injection and retrograde boiling and are therefore locally variable. Nevertheless, only the highly differentiated muscovite-albite pegmatites of the Bergell intrusion contain rare element minerals such as beryl. The internal structure of the dykes and wallrock contact relations suggest that a slow cooling of the dykes lead to their internal layering and zonation.

Nb–Ta mineralizations are strongly dependent on the volatile composition of the fluid. High F and H_2O contents shift the minimum melt composition towards more albitic composition and strongly decrease the solidus temperature (MANNING, 1981). Temperature decrease and Na increase (increase of Na/K ratio) favour albite rock formation and accumulation of tantaloniobates (ALEKSANDROV et al., 1985). This may explain the formation of columbite in the albite rich muscovite pegmatites of the Bergell intrusion. The same authors report that the Ta/Nb ratio increases with high F and decreasing pH. Columbites of the Bergell are high in Nb and low in Ta. This can be explained by a low F fugacity in the pegmatite forming fluid. Thus, the fluid which produced the columbite bearing pegmatite was probably weakly acid, rich in H_2O and CO_2 and low in F. A local exception can be observed in the upper Val Codera where DE MICHELE and ZEZZA (1979) found lepidolite as a reaction product of tourmaline. As deposition of Ta and Nb is favoured by pressure reduction (ALEKSANDROV et al., 1985), this might be the reason for columbite formation by retrograde boiling in the coarse grained pegmatite domains.

The high degree of cation ordering in the investigated columbites is astonishing. Highly ordered ferrocolumbites such as those have not been reported so far in pegmatites elsewhere. Cation ordering may be influenced by the chemical composition of the Nb–Ta phase. Sn together with a high Ta/Nb ratio seems to cause cation disorder. The low Sn and Ta content of the Bergell columbites might be partly responsible for the high degree of cation ordering. Much more important are the pT conditions during crystallization and the subsequent cooling rate. The internal structure of the dykes suggests a slow cooling which is confirmed by the isotope data from VON BLANCKENBURG (1990). These stable geothermal conditions over a long time period could be the main reason for the high degree of cation ordering in the columbite crystals.

Conclusions

a) The acid dykes of the Bergell intrusion are only slightly differentiated pegmatites but can be classified according to their degree of alkali fractionation.

b) The intrusion of the pegmatites produced a alkali metasomatism in wallrock schollen assimilated by the dykes.

c) Crystallization of rare element bearing minerals is restricted to the muscovite pegmatite type rich in albite.

d) Columbite can be found either as small

splinters in a feldspar-quartz matrix or intergrown with garnet, tourmaline and/or beryl of the albite-muscovite pegmatite type.

e) All columbites (with one exception of manganocolumbite) show a similar chemical composition of ferrocolumbite with Mn/Fe ≤ 1[1].

f) The high degree of cation ordering in the columbites is astonishing. Such highly cation ordered ferrocolumbites from pegmatites have not been reported hitherto.

g) Slow postmagmatic cooling rate and the low Sn content of the columbites seem to be responsible for the high degree of cation ordering in the ferrocolumbites of the pegmatites of the Bergell intrusion.

Acknowledgements

We are indebted to R. Maurizio (museum Ciäsa Granda, Stampa), H.A. Stalder and B. Hofmann (museum of natural history, Bern) for providing columbite samples. We highly appreciate the introduction to the Val Bondasca geology by S. Lareida. Ch. Matter and H. Vogel kindly provided helpful field assistance. I. Mercolli is thanked for positive criticism of an earlier version of the manuscript and L. Diamond improved the English. We also acknowledge support of this work by the "Schweizerische Nationalfonds".

References

ALEKSANDROV, I.V., KRASOV, A.M. and KOCHNOVA, L.M. (1985): Effect of potassium, sodium and fluorine on association of rock-forming minerals and formation of tantalum-niobium ore mineralization in rare metal granite pegmatites. Geokhimiya, 620–629.

VON BLANCKENBURG, F.CH. (1990): Isotope geochemical and geochronical case studies of Alpine magmatism and metamorphism: the Bergell intrusion and Tauern Window. Ph. D. thesis, ETH Zürich.

ČERNÝ, P. and ERCIT, T.S. (1989): Mineralogy of niobium and tantalum: crystal chemical relationship, paragenetic aspects and their economic implications. In: MÖLLER, P., ČERNÝ, P. and SAUPÉ, F. (editors). Lanthanides, tantalum and niobium. Soc. Geol. Appl. Min. Spec. publ., 7, 27–80.

DE MICHELE, V. and ZEZZA, U. (1979): Le pegmatiti dell'alta Val Codera. Atti. Soc. ital. Sci. nat. Museo civ. Stor. nat. Milano, 120, 180–194.

DIETHELM, K. (1989): Petrographie und geochemische Untersuchungen an basischen Gesteinen der Bergeller Intrusion. Ph. D. thesis ETH Zürich.

ENRAF NONIUS (1983): Structure determination package (SDP). Enraf Nonius, Delft, Holland.

FERGUSON, R.B., HAWTHORNE, F.C. and GRICE, J.D. (1976): The crystal structure of tantalite, ixiolite and wodginite from Bernic Lake, Manitoba. II Wodginite. Can. Mineral., 14, 550–560.

GRAMACCIOLI, C.M. (1978): Die Mineralien der Alpen, I + II, Ott Verlag, Thun.

GRICE, J.D., FERGUSON, R.B. and HAWTHORNE, F.C. (1976): The crystal structure of tantalite, ixiolite and wodginite from Bernic Lake, Manitoba. I Tantalite and ixiolite. Can. Mineral., 14, 540–549.

GUNTLI, P. and LINIGER, M. (1989): Metamorphose in der Margna-Decke im Bereich Piz da la Margna und Piz Fedoz (Oberengadin). Schweiz. Mineral. Petrogr. Mitt., 69, 289–301.

GYR, T. (1967): Geologische und petrographische Untersuchungen am Ostrande des Bergeller Massivs. Mitt. Geol. Inst. ETH und Uni. Zürich, 66, 1–125.

HALL, S.R. and STEWART, J.N. (1988): XTAL2.4 User's manual. Universities of Western Australia and Maryland.

HAMILTON, W.C. (1959): On the isotropic temperature factor equivalent to a given anisotropic temperature factor. Acta Cryst., 12, 609–611.

HÖLZEL, A.R. (1989): Systematics of minerals. Alexander Hölzel Verlag. Ober-Olm.

LAHTI, S.I. (1987): Zoning in columbite-tantalite crystals from the granitic pegmatites of the Eräjärvi area, southern Finland. Geochim. Cosmochim., 51, 509–517.

LAREIDA, S. (1981): Pegmatite im Bergell. Lapis, Heft 6, 57–59.

MANNING, D.A.C. (1981): The effect of fluorine on liquidus phase relationships in the system Qz–Ab–Or with excess of water at 1 kb. Contrib. Mineral. Petrol, 76, 206–215.

MAURIZIO, R. and SCHATZ, R.H. (1973): Scheelit und Niobit im Bergeller Massiv in der Südostschweiz. Aufschluss, 24, 14–16.

MAURIZIO, R. and LAREIDA, S. (1975): Interessante und noch nicht publizierte Mineralien des Bergells. Mineralienfreund, Heft 1, 65–74.

MAURIZIO, R. and WEIBEL, M. (1982): Die Mineralien des Bergells. Mineralienfreund, 4, 81–100.

MOTICSKA, P. (1970): Petrographie und Strukturanalyse des westlichen Bergeller Massivs und seines Rahmens. Schweiz. Mineral. Petrogr. Mitt., 50, 355–443.

MÖLLER, P. (1989): REE(Y), Nb, and Ta enrichment in pegmatites and carbonatite-alkalic rock complexes. In: MÖLLER, P., ČERNÝ, P. and SAUPÉ, F. (editors). Lanthanides, tantalum and niobium. Soc. Geol. Appl. Min. Spec. publ., 7, 103–144.

NICKEL, E.H., ROWLAND, J.F. and MCADAM, R.C. (1963): Ixiolite – a columbite substructure. Amer. Mineral., 48, 961–979.

PEREGO, G. (1979): Itinerari mineralogici Val Masino e Bassa Valtellina. Com. Monatana, Sondrio.

REUSSER, E. (1987): Phasenbeziehungen im Tonalit der Bergeller Intrusion (Graubünden, Schweiz / Provinz Sondrio, Italien). Ph. D. thesis ETH Zürich.

SCHMUTZ, H.U. (1976): Der Mafitit-Ultramafitit-Komplex zwischen Chiavenna und Val Bondasca. Beitr. Geol. Karte der Schweiz, 149, 1–73.

[1] A reinvestigation of an ixiolite and a manganotantalite sample reported from different authors, disclosed the ixiolite as titanohematite and the manganotantalite as an X-ray amorphous iron bearing silicate. Thus, all Nb,Ta-oxides of the ixiolite-columbite-tantalite group reported from pegmatites of the Bergell intrusion are iron rich columbites.

SCHOMAKER, V. and MARSH, R.E. (1983): On evaluating the standard deviation of U_{eq}. Acta Cryst., A39, 819–820.

SIMMONS, W.B., LEE, M.T. and BREWSTER, R.H. (1987): Geochemistry and evolution of the South Platte granite-pegmatite system, Jefferson County, Colorado. Geochim. Cosmochim., 51, 455–472.

STAUB, R. (1921): Geologische Karte der Val Bregaglia (Bergell). Geol. Spezialkarten der Schweiz, Blatt 90.

STAUB, R. (1924): Zur Kenntnis der Bergeller Berylle. Schweiz. Mineral. Petrogr. Mitt., 4, 364–367.

STERN, W.B. (1972): Zur röntgenspektrometrischen Analyse von silikatischen Gesteinen und Mineralien. Schweiz. Mineral. Petrogr. Mitt., 52, 1–27.

TROMMSDORFF, V. and NIEVERGELT, P. (1983): The Bregaglia (Bergell) Iorio intrusive and its field relations. Mem. Soc. Geol. It., 26, 55–68.

TRÖGER, W.E. (1982): Optische Bestimmung der gesteinsbildenden Minerale. Teil 1. Bestimmungstabellen. E. Schweizerbart'sche Verlagsbuchhandlung, Stuttgart.

UYTENBOGAARDT, W. and BURKE, E.A.J. (1971): Tables for microscopic identification of ore minerals. Elsevier Publishing Company. Amsterdam.

VOGLER, K. (1982): Petrographie und Mineralogie von Pegmatiten und ihren Nebengesteinen im Gebiete des Pizzo Trubinasca. Master thesis Univ. Basel.

WEITZEL, H. (1976): Kristallstrukturverfeinerung von Wolframiten und Columbiten. Z. Krist., 144, 238–258.

WENGER, M., ARMBRUSTER, TH. and GEIGER, C.A. (1991): Cation distribution in partially ordered columbite from the Kings Mountain pegmatite, N.C. Amer. Mineral., 76, 1877–1884.

WENK. H.R. and CORNELIUS, S.B. (1977): Geologischer Atlas der Schweiz. 1:25 000, Blatt 70, Sciora. Schweiz. Geol. Komm.

WENK, H.R., HSIAO, J., FLOWERS, G., WEIBEL, M., AYRANCI, B. and FEJÉR, Z. (1977): A geochemical survey of granitic rocks in the Bergell Alps. Schweiz. Mineral. Petrogr. Mitt., 57, 233–265.

WENK, H.R. (1986): Introduction to the geology of the Bergell Alps with guide for excursions. Jahresber. Naturforsch. Gesell. Graubünden, 103, 29–90.

Manuscript received May 10, 1991; revised manuscript accepted August 16, 1991.